PROCEEDINGS OF SCIENCE

Light meson spectrum with $N_f = 2+1$ dynamical overlap fermions

JLQCD and TWQCD collaborations: J. Noaki[*,a†], S. Aoki[b,c], T.W. Chiu[d], H. Fukaya[a,e], S. Hashimoto[a,f], T.H. Hsieh[g], T. Kaneko[a,f], H. Matsufuru[a], T. Onogi[h], E. Shintani[a] and N. Yamada[a,f]

[a] *High Energy Accelerator Research Organization (KEK), Tsukuba 305-0801, Japan*
[b] *Graduate School of Pure and Applied Sciences, University of Tsukuba, Tsukuba 305-8571, Japan*
[c] *Riken BNL Research Center, Brookhaven National Laboratory, Upton, NY 11973, USA*
[d] *Physics Department, Center for Theoretical Sciences, and Center for Quantum Science and Engineering, National Taiwan University, Taipei 10617, Taiwan*
[e] *The Niels Bohr Institute, The Niels Bohr International Academy, Blegdamsvej 17 DK-2100 Copenhagen Ø, Denmark*
[f] *School of High Energy Accelerator Science, the Graduate University for Advanced Studies (Sokendai), Tsukuba 305-0801, Japan*
[g] *Research Center for Applied Sciences, Academia Sinica, Taipei 115, Taiwan*
[h] *Yukawa Institute for Theoretical Physics, Kyoto University, Kyoto 606-8502, Japan*

We report on a numerical simulation with 2+1 dynamical flavors of overlap fermions. We calculate pseudo-scalar masses and decay constants on a $16^3 \times 48 \times (0.11\ \mathrm{fm})^4$ lattice at five different up and down quark masses and two strange quark masses. The lightest pion mass corresponds to ≈ 310 MeV. We also study the validity of the chiral perturbation theory using the results of the numerical simulation with two dynamical flavors and conclude that the one-loop formulae cannot be directly applied in the strange quark mass region. We therefore extrapolate our 2+1-flavor results to the chiral limit by fitting the data to the two-loop formulae of the chiral perturbation theory.

The XXVI International Symposium on Lattice Field Theory
July 14-19 2008
Williamsburg, Virginia, USA

[*]Speaker.
[†]E-mail: noaki@post.kek.jp

PoS(LATTICE 2008)107

1. Introduction

The lattice simulation with the overlap fermions [1] provides a theoretically ideal setup to study low energy hadron physics. With the exact chiral symmetry, the continuum chiral perturbation theory (ChPT) can be applied without modification in sharpe contrast to other fermion formulations that violate either chiral or flavor symmetry. For this advantage, we performed numerical simulation using overlap fermion action with two dynamical flavors [2]. In particular, we carried out the calculation of light meson spectrum and studied the consistency between QCD and chiral perturbation theory. In this article, we present an extension of this study to the $N_f = 2+1$ QCD similar parameters. On a $16^3 \times 48$ lattice, we generate 2,500 trajectories [4, 5] at ten different combinations of up/down and strange sea quark masses, *i.e.* five m_{ud}'s and two m_s's. As in the $N_f = 2$ case, topological charge of the gauge configuration is fixed to zero throughout Monte Carlo updates. Lattice spacing is determined by the Sommer scale as $a = 0.1075(7)$ fm or $a^{-1} = 1.833(12)$ GeV from an input $r_0 = 0.49$ fm.

In section 2, we present basic part of the calculation of pseudo-meson masses and decay constants. Since these results depend on strange quark mass, the chiral extrapolation should be performed with a fit ansatz valid beyond the scale of kaon mass. To discuss this issue, we review the test of ChPT performed for the $N_f = 2$ case in section 3. Based on this test, in section 4, we present the extrapolation of the $N_f = 2+1$ data by using the two-loop ChPT formulae.

2. Spectrum calculation ($N_f = 2+1$)

For the $N_f = 2+1$ case, we calculate 80 pairs of the lowest-lying eigenmodes on each gauge configuration and store them on the disks. These eigenmodes are used to construct the low-mode contribution to the quark propagators. The higher-mode contribution is obtained by conventional CG calculation with significantly smaller amount of machine time than the full CG calculation. Those eigenmodes are also used to replace the lower-mode contribution in the meson correlation functions by that averaged over the source location (low-mode averaging) [6, 7]. The noise of correlation function is decreased as shown in Figure 1, where effective pion masses are compared between the data with and without the low-mode averaging for the lightest four quark masses.

In order to obtain renormalization factor of quark mass Z_m, we calculate scalar and pseudoscalar vertex functions in the momentum space in the Landau gauge and applied the RI/MOM scheme [8]. In the fit of the vertex functions we explicitly use the low-mode contribution to the chiral condensate

$$\langle \bar{q}q \rangle (m_q) = \left\langle \frac{1}{V} \sum_{i=1}^{80} \frac{2m_q}{m_q^2 + \lambda_i^2} \right\rangle \tag{2.1}$$

with eigenvalues λ_i and absorb its valence quark mass dependence. By converting $Z_m^{\mathrm{RI/MOM}}$ in the massless limit into the value of $\overline{\mathrm{MS}}$ perturbatively, we obtain a preliminary value $Z_m^{\overline{\mathrm{MS}}}(2\,\mathrm{GeV}) = 0.815(8)$.

On our lattice with spatial extent L, the lightest pion gives $m_\pi L \approx 2.8$. Finite size effect (FSE) may therefore be sizable. We estimate this effect using the analytic result [9] from a combination of the resummed Lüscher's formulae and an one-loop ChPT. There is an additional finite size due

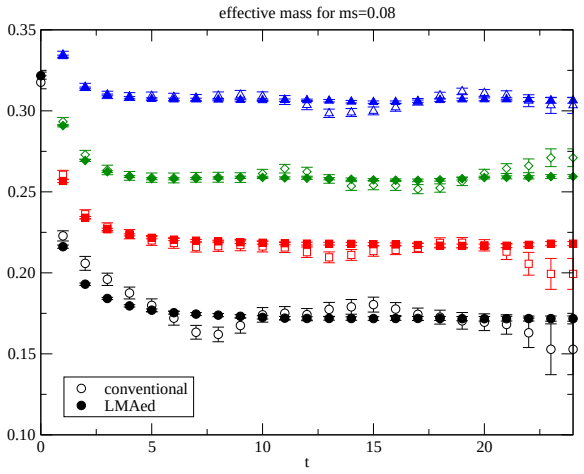

Figure 1: Effective pion mass plots for the four lightest quark mass. Open symbols indicate signals from conventional treatment while filled symbols are from low-mode-averaging.

to the fixed topology in our numerical simulation [10]. Based on the discussion in [11], we make a correction using the result of one-loop ChPT and the numerical data of topological susceptibility [12] determined on the same lattice configurations.

3. Chiral extrapolation ($N_f = 2$)

We address the validity of the NLO ChPT prediction which is commonly used in the chiral extrapolation of spectrum data on the lattice [3]. In the framework of $N_f = 2$, pion mass and decay constants are expanded in terms of $x = 4Bm_q/(4\pi f)^2$ as

$$m_\pi^2/m_q = 2B(1+\tfrac{1}{2}x\ln x) + c_3 x, \tag{3.1}$$

$$f_\pi = f(1 - x\ln x) + c_4 x \tag{3.2}$$

to NLO (*i.e.* one-loop level or $\mathcal{O}(x)$), where B and f are the tree level low energy constants (LECs), and c_3 and c_4 are related to the one-loop level LECs $\bar{l}_3$ and $\bar{l}_4$. At NLO, these expressions are unchanged when one replaces the expansion parameter x by $\hat{x} = 2m_\pi^2/(4\pi f)^2$ or $\xi = 2m_\pi^2/(4\pi f_\pi)^2$, where m_π^2 and f_π denote those at a finite quark mass. Therefore, in a small enough pion mass region the three expansion parameters should describe the lattice data equally well.

Three fit curves (x-fit, $\hat{x}$-fit and ξ-fit) for the three lightest pion mass points ($m_\pi \lesssim 450$ MeV) are shown in Figure 2 as a function of m_π^2. For all fits, the horizontal axis is appropriately rescaled to give m_π^2 using the obtained fit curves.

From the plot we observe that the different expansion parameters describe the three lightest points equally well; the values of χ^2/dof are 0.30, 0.33 and 0.66 for x-, $\hat{x}$- and ξ-fits, respectively. In each fit, the correlation between m_π^2/m_q and f_π for common sea quark mass is taken into account. Between the x- and $\hat{x}$-fit, all of the resulting fit parameters are consistent. Among them, B and f are also consistent with the ξ-fit. This indicates that the NLO formulae successfully describes the data. In Figure 3, results of B (upper panel) and f (bottom panel) for different fits are plotted for different

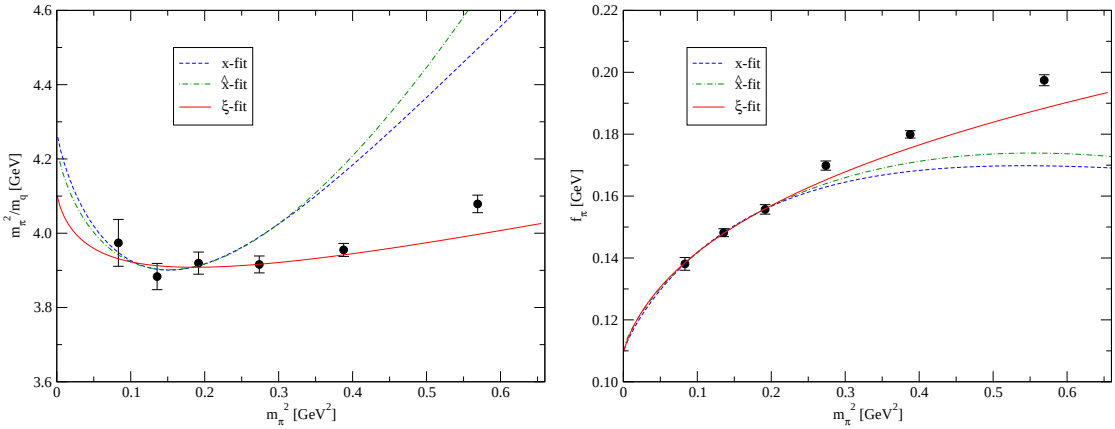

Figure 2: Comparison of the chiral fits including the NLO terms for m_π^2/m_q (left) and f_π (right) obtained in the $N_f = 2$ calculation. Fit curves for the three lightest data points obtained with different choices of the expansion parameter (x, $\hat{x}$ and ξ) are shown as a function of m_π^2.

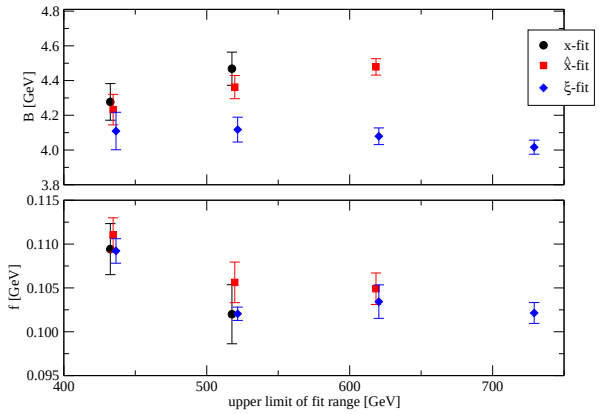

Figure 3: Results of fit parameters B (top) and f (bottom) as functions of the upper limit of the fit range. In each panel, circle, square and diamonds are obtained with fit parameters x, $\hat{x}$ and ξ. Results with $\chi^2/\mathrm{dof} \lesssim 2$ are plotted.

pion mass points. As seen in the figure, the agreement among the different expansion prescriptions is lost when we extend the fit range to include the 4th lightest data point which corresponds to $m_\pi \simeq$ 520 MeV. We, therefore, conclude that for these quantities the NLO ChPT may be safely applied only below $\approx$ 450 MeV.

Another important observation from Figure 2 is that only the ξ-fit reasonably describes the data beyond the fitted region. With the x- and $\hat{x}$-fits the curvature due to the chiral logarithm is too strong to accommodate the heavier data points. In fact, values of the LECs with the x- and $\hat{x}$-fits are more sensitive to the fit range than the ξ-fit. This is because f, which is significantly smaller than f_π of our data, enters in the definition of the expansion parameter. Qualitatively, by replacing m_q and f by m_π^2 and f_π the higher loop effects in ChPT are effectively resummed and the convergence of the chiral expansion is improved.

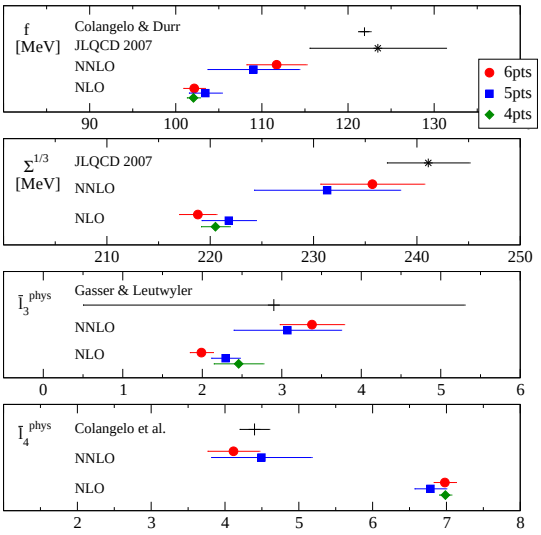

Figure 4: Comparison of the $N_f = 2$ results from the NLO fit and the NNLO fit with ξ. Black pluses denote reference points from phenomenological estimations.

We then extend the analysis to include the NNLO terms [13]. Since we found that only the ξ-fit reasonably describes the data beyond $m_\pi \simeq 450$ MeV, we perform the NNLO analysis using the ξ-expansion. Although we input phenomenological estimate of LECs $\bar{l}_1$ and $\bar{l}_2$, we find our fit result is insensitive to their uncertainties. We extract the LECs of ChPT, *i.e.* the decay constant in the chiral limit f, chiral condensate $\Sigma = Bf^2/2$, and the NLO LECs $\bar{l}_3^{\rm phys} = -c_3/B + \ln(2\sqrt{2}\pi f/m_{\pi^+})^2$ and $\bar{l}_4^{\rm phys} = c_4/f + \ln(2\sqrt{2}\pi f/m_{\pi^+})^2$. For each quantity, a comparison of the results between the NLO and the NNLO fits is shown in Figure 4. In each panel, the results with 5 and 6 lightest data points are plotted for the NNLO fit. The correlated fits give $\chi^2/\mathrm{dof} = 1.94$ and 1.40, respectively. For the NLO fits, we plot results obtained with 4, 5 and 6 points to show the stability of the fit. The χ^2/dof is less than 1.94. The results for these physical quantities are consistent within either the NLO or the NNLO fit. On the other hand, as seen for $\bar{l}_4^{\rm phys}$ most prominently, there is a significant disagreement between NLO and NNLO. This is due to the large NNLO contributions to the terms which are proportional to c_3 and c_4, respectively.

We quote our final results for the $N_f = 2$ calculation from the NNLO fit with all data points: $f = 111.7(3.5)(1.0)(^{+6.0}_{-0.0})$ MeV, $\Sigma^{\overline{\rm MS}}(2\ \mathrm{GeV}) = [235.7(5.0)(2.0)(^{+12.7}_{-\ 0.0})\ \mathrm{MeV}]^3$, $\bar{l}_3^{\rm phys} = 3.38(40)(24)(^{+31}_{-\ 0})$, and $\bar{l}_4^{\rm phys} = 4.12(35)(30)(^{+31}_{-\ 0})$, where $m_\pi^+ = 139.6$ MeV. From the value at the neutral pion mass $m_{\pi^0} = 135.0$ MeV, we obtain the average up and down quark mass m_{ud} and the pion decay constant as $m_{ud}^{\overline{\rm MS}}(2\ \mathrm{GeV}) = 4.452(81)(38)(^{+\ 0}_{-227})$ MeV and $f_\pi = 119.6(3.0)(1.0)(^{+6.4}_{-0.0})$ MeV. In these results, the first error is statistical, where the error of the renormalization constant is included in quadrature for $\Sigma^{1/3}$ and m_{ud}. The second error is systematic due to the truncation of the higher order corrections. For quantities carrying mass dimensions, the third error is from the ambiguity in the determination of r_0. We estimate these errors from the difference of the results with our input $r_0 = 0.49$ fm and that with 0.465 fm. The third errors for $\bar{l}_3^{\rm phys}$ and $\bar{l}_4^{\rm phys}$ reflect an ambiguity of choosing the renormalization scale of ChPT ($4\pi f$ or $4\pi f_\pi$).

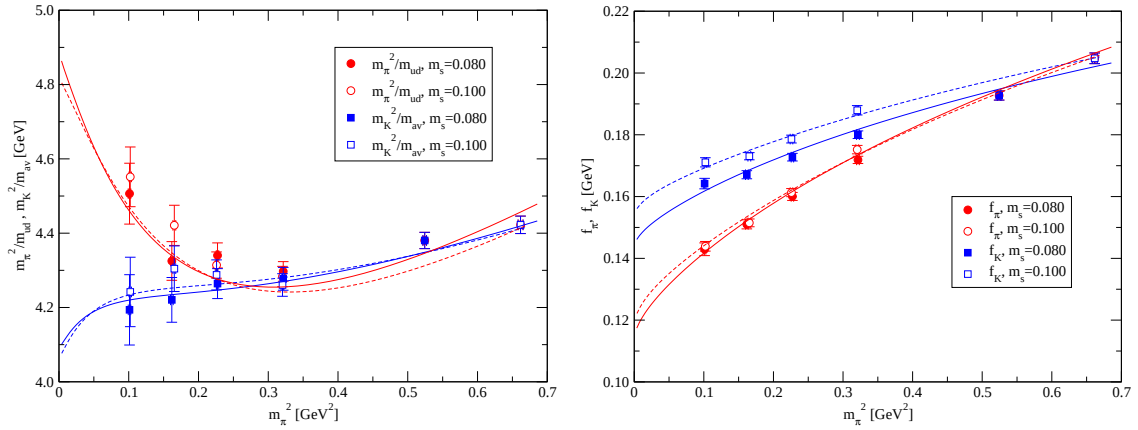

Figure 5: Chiral properties of m_π^2/m_{ud} and m_K^2/m_{av} (left) and f_π and f_K (right) for fixed values of strange quark mass (open and filled symbols). In each panel, circles (squares) indicate the pion (kaon) data.

4. Chiral extrapolation ($N_f = 2+1$)

Since we found in the two-flavor calculation that the NNLO ChPT formulae can nicely fit our data even in the kaon mass region if one uses the ξ-expansion, we apply the same strategy for our $2+1$-flavor analysis.

As functions of $\xi_\pi = m_\pi^2/(4\pi f_\pi)^2$ and $\xi_{\eta_s} = m_{\eta_s}^2/(4\pi f_\pi)^2$, where η_s is the unphysical strange-strange meson, chiral expansions are expressed as

$$m_\pi^2/m_{ud} = 2B_0(1+M^\pi(\xi_\pi,\xi_{\eta_s};L_i^r)) + \alpha_1^\pi\xi_\pi^2 + \alpha_2^\pi\xi_\pi\xi_{\eta_s} + \alpha_3^\pi\xi_{\eta_s}^2 \quad (4.1)$$

$$m_K^2/m_{av} = 2B_0(1+M^K(\xi_\pi,\xi_{\eta_s};L_i^r)) + \alpha_1^K\xi_\pi(\xi_\pi-\xi_{\eta_s}) + \alpha_2^K\xi_{\eta_s}(\xi_{\eta_s}-\xi_\pi) \quad (4.2)$$

$$f_\pi = f_0(1+F^\pi(\xi_\pi,\xi_{\eta_s};L_i^r)) + \beta_1^\pi\xi_\pi^2 + \beta_2^\pi\xi_\pi\xi_{\eta_s} + \beta_3^\pi\xi_{\eta_s}^2 \quad (4.3)$$

$$f_K = f_0(1+F^K(\xi_\pi,\xi_{\eta_s};L_i^r)) + \beta_1^K\xi_\pi(\xi_\pi-\xi_{\eta_s}) + \beta_2^K\xi_{\eta_s}(\xi_{\eta_s}-\xi_\pi), \quad (4.4)$$

where $m_{av} = \frac{1}{2}(m_s+m_{ud})$ and $\alpha_i^{\pi,K}$ and $\beta_i^{\pi,K}$ are NNLO unknown parameters. Functions M^π, M^K, F^π and F^K contain NLO contributions and loop contributions at NNLO, whose expressions are too involved to present here [14]. Among relevant SU(3) LECs L_1^r–L_8^r, we use values $L_1^r = (0.38\pm0.18)\cdot10^{-3}$, $L_2^r = (1.59\pm0.15)\cdot10^{-3}$, $L_3^r = (-2.91\pm0.32)\cdot10^{-3}$ and $L_7^r = (-0.49\pm0.24)\cdot10^{-3}$ (defined at $\mu = 770$ MeV) from a phenomenological estimate [15] and determine others by a fit. Thus, the chiral extrapolation with (4.1)–(4.4) contains 16 fit parameters in total. We fit m_π^2/m_{ud}, m_K^2/m_{av}, f_π and f_K simultaneously taking the correlation between these quantities at the same sea quark mass (m_{ud}, m_s) into account. By using all data points, χ^2/dof = 1.42 is obtained. Data after the finite size corrections are shown in Figure 5 as a function of m_π^2. Different symbols correspond to the pion data (m_π^2/m_{ud} and f_π) and the kaon data (m_K/m_{av} and f_K) while the filled (open) pattern represent a fixed lighter (heavier) strange quark mass, which is accompanied by the solid (dashed) curves.

Extrapolating the data to the physical point $m_\pi = 135.0$ MeV, $m_K = 495.0$ MeV and $f_\pi = 130.7$ MeV, we obtain preliminary results $m_{ud}^{\overline{\rm MS}}(2\,{\rm GeV}) = 3.799(68)$ MeV, $m_s^{\overline{\rm MS}}(2\,{\rm GeV}) = 114.6(2.0)$ MeV, $f_\pi = 121.5(4.1)$ MeV, $f_K = 148.3(4.7)$ MeV and $f_K/f_\pi = 1.220(10)$, where the errors are statisti-

cal only. Further studies to determine LECs and to analyze their flavor dependence are planned as well as the estimation of systematic errors.

Numerical simulations are performed on Hitachi SR11000 and IBM System Blue Gene Solution at High Energy Accelerator Research Organization (KEK) under a support of its Large Scale Simulation Program (No. 07-16). This work is supported in part by the Grant-in-Aid of the Ministry of Education (Nos. 18340075, 18740167, 19540286, 19740121, 19740160, 20025010, 20039005, 20340047, 20740156), the National Science Council of Taiwan (Nos. NSC96-2112-M-002-020-MY3, NSC96-2112-M-001-017-MY3, NSC97-2119-M-002-001) and NTU-CQSE (No. 97R0066-69).

References

[1] H. Neuberger, Phys. Lett. **B427** (1998) 353 [arXiv:hep-lat/9801031].

[2] JLQCD Collaboration (S. Aoki *et al*), Phys. Rev. D **78** (2008) 014508, [arXiv:0803.3197 [hep-lat]].

[3] JLQCD and TWQCD Collaborations (J. Noaki *et al*), arXiv:0806.0894 [hep-lat].

[4] S. Hashimoto, in these proceedings.

[5] JLQCD and TWQCD Collaborations (H. Matsufuru *et al*), in these proceedings.

[6] T. DeGrand and S. Schaefer, Comp. Phys. Comm. **159** (2004) 185, [arXiv:hep-lat/0401011].

[7] L. Giusti, P. Hernández, M. Laine, P. Weisz, H. Wittig, JHEP **04** (2004) 013, [arXiv:hep-lat/0402002].

[8] G. Martinelli, C. Pittori, C. T. Sachrajda, M. Testa and A. Vladikaa, Nucl. Phys. **B445** (1995) 81, [arXiv:hep-lat/9411010].

[9] G. Colangelo, S. Dürr and C. Haefeli, Nucl. Phys. **B721** (2005) 136, [arXiv:hep-lat/0503014].

[10] R. Brower, S. Chandrasekharan, J. W. Negele and U.-J. Wiese, Phys. Lett. **B560** (2003) 64, [arXiv:hep-lat/0302005].

[11] S. Aoki, H. Fukaya, S. Hashimoto and T. Onogi, Phys. Rev. D **76** (2007) 054508, [arXiv:0707.0396 [hep-lat]].

[12] JLQCD and TWQCD Collaborations (T.W. Chiu *et al.*), in these proceedings.

[13] G. Colangelo, J. Gasser and H. Leutwyler, Nucl. Phys. **B603** (2001) 125, [arXiv:hep-ph/0103088].

[14] G. Amorós, J. Bijnens and P. Talavera, Nucl. Phys. **B568** (2000) 319, [arXiv:hep-ph/9907264] ; We thank J. Bijnens for providing his Fortran code evaluating the contribution of sunset integrals among the two-loop effects.

[15] G. Amorós, J. Bijnens and P. Talavera, Nucl. Phys. **B602** (2001) 87, [arXiv:hep-ph/0101127].